Hemagglutinin–neuraminidase balance confers respiratory-droplet transmissibility of the pandemic H1N1 influenza virus in ferrets

Hui-Ling Yen[a,b], Chi-Hui Liang[c], Chung-Yi Wu[c], Heather L. Forrest[d], Angela Ferguson[d], Ka-Tim Choy[a], Jeremy Jones[d], Diana Dik-Yan Wong[a], Peter Pak-Hang Cheung[a], Che-Hsiung Hsu[c], Olive T. Li[a], Kit M. Yuen[a], Renee W. Y. Chan[a,e], Leo L. M. Poon[a], Michael C. W. Chan[a], John M. Nicholls[e], Scott Krauss[d], Chi-Huey Wong[c], Yi Guan[a], Robert G. Webster[d,1], Richard J. Webby[d], and Malik Peiris[a,b,1]

[a]Department of Microbiology, [b]HKU–Pasteur Research Centre, and [e]Department of Pathology, University of Hong Kong, Pokfulam, Hong Kong SAR, China; [c]Genomics Research Center, Academia Sinica, Taipei 115, Taiwan; and [d]Division of Virology, Department of Infectious Diseases, St. Jude Children's Research Hospital, Memphis, TN 38105

Contributed by Robert G. Webster, July 11, 2011 (sent for review April 15, 2011)

A novel reassortant derived from North American triple-reassortant (TRsw) and Eurasian swine (EAsw) influenza viruses acquired sustained human-to-human transmissibility and caused the 2009 influenza pandemic. To identify molecular determinants that allowed efficient transmission of the pandemic H1N1 virus among humans, we evaluated the direct-contact and respiratory-droplet transmissibility in ferrets of representative swine influenza viruses of different lineages obtained through a 13-y surveillance program in southern China. Whereas all viruses studied were transmitted by direct contact with varying efficiency, respiratory-droplet transmissibility (albeit inefficient) was observed only in the TRsw-like A/swine/Hong Kong/915/04 (sw915) (H1N2) virus. The sw915 virus had acquired the M gene derived from EAsw and differed from the gene constellation of the pandemic H1N1 virus by the neuraminidase (NA) gene alone. Glycan array analysis showed that pandemic H1N1 virus A/HK/415742/09 (HK415742) and sw915 possess similar receptor-binding specificity and affinity for α2,6-linked sialosides. Sw915 titers in differentiated normal human bronchial epithelial cells and in ferret nasal washes were lower than those of HK415742. Introducing the NA from pandemic HK415742 into sw915 did not increase viral replication efficiency but increased respiratory-droplet transmissibility, despite a substantial amino acid difference between the two viruses. The NA of the pandemic HK415742 virus possessed significantly higher enzyme activity than that of sw915 or other swine influenza viruses. Our results suggest that a unique gene constellation and hemagglutinin–neuraminidase balance play a critical role in acquisition of efficient and sustained human-to-human transmissibility.

influenza A | zoonosis | viral genes

A novel H1N1 influenza virus that emerged through reassortment of swine influenza viruses caused the 2009 influenza pandemic. The virus contained a unique gene constellation, deriving six gene segments from the North American "triple-reassortant" swine (TRsw) and its neuraminidase (NA) and M genes from the "Eurasian" swine (EAsw) influenza viruses (1, 2). The TRsw influenza viruses emerged in the late 1990s through reassortment between classical swine (Csw) (descended from the 1918 pandemic virus), avian, and human influenza viruses (3, 4). The EAsw influenza viruses were of avian origin that became established in European swine in the late 1970s (5, 6). Although sporadic zoonotic infection with swine influenza viruses (7, 8) and reverse zoonosis of human seasonal influenza viruses in swine herds (9) have been reported, sustained human-to-human transmission of swine influenza viruses was not documented until the 2009 pandemic. To understand the mechanism of the emergence of influenza pandemicity, it is essential to identify viral determinants that confer efficient transmission in humans.

Previous studies identified hemagglutinin (HA) receptor-binding specificity for α2,6-linked sialic acids (10, 11) and the ability to replicate at 33 °C (as conferred by residues K627 and N701 in PB2) (12, 13) as molecular determinants of efficient respiratory-droplet transmissibility in ferrets, an animal model that closely resembles human influenza infection. Introducing K627 or N701 into PB2 of the swine-origin pandemic H1N1 virus (which possesses E627 and D701) did not affect viral pathogenicity or transmissibility in animal models (14, 15). Furthermore, glycan array analysis revealed preferential binding to α2,6-linked sialyl glycans in both the pandemic H1N1 (16–19) and the H1-subtype swine influenza viruses (17, 20–22), suggesting subtle changes in HA were not the key determinants for the 2009 H1N1 virus pandemicity. In addition to the known molecular markers, a second-site suppressor polymorphism in the PB2 subunit of the 2009 pandemic H1N1 influenza virus has been proposed to mediate efficient replication in humans (23); however, its effect on viral transmissibility has not been directly tested.

We have systematically conducted prospective surveillance of swine influenza in southern China over the past 13 y (2, 24, 25). Until 2002, the predominant H1 viruses circulating in swine were Csw-like viruses; since 2002, North American TRsw-like and avian-origin EAsw-like viruses have cocirculated with Csw-like viruses, and reassortants between these lineages have been detected (2, 24, 25). The availability of swine influenza viruses of different lineages and of natural reassortants from these lineages provided an opportunity to investigate the viral genetic determinants of the human transmissibility of the pandemic virus. We assessed direct-contact and respiratory-droplet transmissibility of pandemic H1N1 viruses and representative swine influenza viruses of the H1N1 or H1N2 subtypes in a ferret model. Plasmid-based reverse genetics was applied to identify gene segments that confer efficient respiratory-droplet transmissibility. Overall, our results suggest that the unique gene constellation and the HA–NA balance were the key determinants of the efficient human transmissibility of pandemic H1N1 viruses.

Results

Transmission of Pandemic H1N1 and Swine Influenza Viruses in Ferrets. We first compared the direct-contact and respiratory-droplet transmission efficiency of pandemic H1N1 viruses A/California/4/09 (CA04) and HK415742 to that of a recombinant seasonal H3N2 influenza virus, A/Wuhan/359/95 (Wuhan95) (Fig. 1 *A* and *B*). The

Author contributions: H.-L.Y. and M.P. designed research; H.-L.Y., C.-H.L., C.-Y.W., H.L.F., A.F., K.-T.C., J.J., D.D.-Y.W., P.P.-H.C., C.-H.H., O.T.L., K.M.Y., R.W.Y.C., L.L.M.P., M.C.W.C., J.M.N., and S.K. performed research; C.-Y.W., C.-H.W., and Y.G. contributed new reagents/analytic tools; H.-L.Y., C.-H.L., C.-Y.W., and M.P. analyzed data; and H.-L.Y., C.-Y.W., R.G.W., R.J.W., and M.P. wrote the paper.

The authors declare no conflict of interest.

[1]To whom correspondence may be addressed. E-mail: robert.webster@stjude.org or malik@hkucc.hku.hk.

This article contains supporting information online at www.pnas.org/lookup/suppl/doi:10.1073/pnas.1111000108/-/DCSupplemental.

area under the curve (AUC) estimated the total quantity of virus shed. After inoculation with 10^5 $TCID_{50}$ (50% tissue culture infectious dose) of virus, donor ferrets had a similar mean AUC for Wuhan95 and HK415742 viruses but a slightly lower AUC for CA04 virus ($P < 0.05$, one-way ANOVA and Tukey's test) (Table S1). The pandemic viruses were transmitted to all three direct-contact ferrets with an efficiency similar to that of Wuhan95 virus. Direct-contact animals in the three virus groups shed a similar quantity of virus, with peak titers at 4 d postinoculation (dpi). Ferrets infected by respiratory-droplet contact also had comparable AUCs for the pandemic and seasonal viruses; however, peak titers were detected earlier for Wuhan95 (4 and 6 dpi) than for pandemic HK415742 (6 and 8 dpi) and CA04 (6, 6, and 10 dpi) (Fig. 1*B*). As a result, animals infected with pandemic H1N1 via respiratory droplets shed virus longer (to 12 dpi) (Fig. 1*B*). The pandemic viruses caused greater weight loss than did Wuhan95 (Table S2). Overall, these results suggest that the pandemic and seasonal viruses are similarly transmissible by direct contact, whereas the pandemic viruses are transmitted slightly less efficiently by respiratory droplets.

We next evaluated the transmissibility of swine influenza viruses of the pandemic precursor lineages, including A/Sw/HK/4167/99 (sw4167, Csw-lineage), A/Sw/HK/NS29/09 (swNS29, EAsw-lineage), and A/Sw/Arkansas/2976/02 (swAR2976, TRsw-lineage) (Fig. 1*C*). Two natural reassortants between the TRsw and EAsw (sw915 and A/Sw/HK/201/10; sw201) were assessed as well (Fig. 1*D*). Sw915 is a TRsw-like virus that acquired the M gene from the EAsw lineage (2). Sw201, isolated after the emergence of the 2009 pandemic, contained the TRsw internal genes, the EAsw HA gene, and the pandemic H1N1 virus NA gene (24).

All donor ferrets inoculated with the swine influenza viruses shed comparable quantities of virus, with the exception of those inoculated with sw915, which shed less virus ($P < 0.05$, one-way ANOVA and Tukey's test) than those inoculated with swAR2976, sw4167, or sw201 (Table S1). All swine influenza viruses were transmitted by direct contact, albeit with different efficiency (Fig. 1 *C* and *D*). SwAR2976 and sw201 viruses were more efficiently transmitted by direct contact, as virus was detected from naïve direct-contact ferrets by 4 dpi; sw4167 and sw915 were transmitted at moderate efficiency, with viruses detected by 6 dpi. The EAsw-like swNS29 was transmitted least efficiently by direct contact, as virus was shed by only 2/3 direct-contact ferrets by 8 dpi; the uninfected ferret remained seronegative 18 d postcontact (Table S3). Ferrets inoculated with the swNS29 virus also lost less weight (Table S2). Peak titers occurred consistently earlier in direct-contact ferrets infected with seasonal or pandemic H1N1 virus (4 dpi) versus swine virus (4–8 dpi) (Fig. 1).

Unlike the pandemic H1N1 viruses, the swine influenza viruses studied were not efficiently transmitted by respiratory droplets. However, sw915 was detected in 1/5 respiratory-droplet contacts by 8 dpi (Fig. 1*D*). One respiratory-droplet contact in the swNS29 group showed seroconversion without detectable virus shedding (Table S3).

Minigenome Assay and Replication Kinetics of Recombinant Influenza Viruses. We observed the sw915 virus was transmitted inefficiently by respiratory droplets. To identify molecular determinants of efficient respiratory-droplet transmission of the pandemic H1N1 virus, we used sw915 as the backbone and introduced gene segments from the pandemic H1N1 virus HK415742. Sequence analysis showed that sw915 and HK415742 differed by 114 amino acids in the seven phylogenetically related genes (Table S4).

As the polymerase complex is known to play a role in respiratory-droplet transmission (13), we first evaluated the transcription and replication efficiency of the polymerase complex in human 293T cells by using a viral RNA-like reporter plasmid (*SI Materials and Methods*). The polymerase complex of HK415742 showed higher activity than that of sw915 at both 37 °C and 33 °C (Fig. 2*A*). Replacing the PB2 and PA of sw915 with those of HK415742 increased sw915 polymerase activity; replacing the nucleoprotein (NP) of HK415742 with that of sw915 increased HK415742 polymerase activity (Fig. 2*A*). These results suggested that the PB2 and PA of HK415742 may contribute to higher polymerase transcription and replication efficiency.

The replication kinetics of the recombinant viruses were examined in Madin–Darby canine kidney (MDCK) cells and differentiated normal human bronchial epithelial (dNHBE) cells. As seven of the eight gene segments of sw915 are phylogenetically closely related to the pandemic H1N1 virus, we first replaced the NA of sw915 with that of HK415742 to generate the RG-sw915xHK415742^{NA} virus. As the HA of sw915 and HK415742 differed by 26 amino acids (including three located at antigenic sites and two near the receptor-binding domain) (Table S4), the RG-sw915xHK415742^{HA,NA} virus was generated to assess the effect of HA–NA balance on viral fitness. To address the role of the polymerase complex, we generated RG-sw915xHK415742^{PB2,PA} and RG-sw915xHK415742^{PB2,PA,HA,NA} viruses. RG-sw915 and RG-HK415742 were generated for comparison. Heterogeneous plaque morphology was observed occasionally (Fig. S1) after two

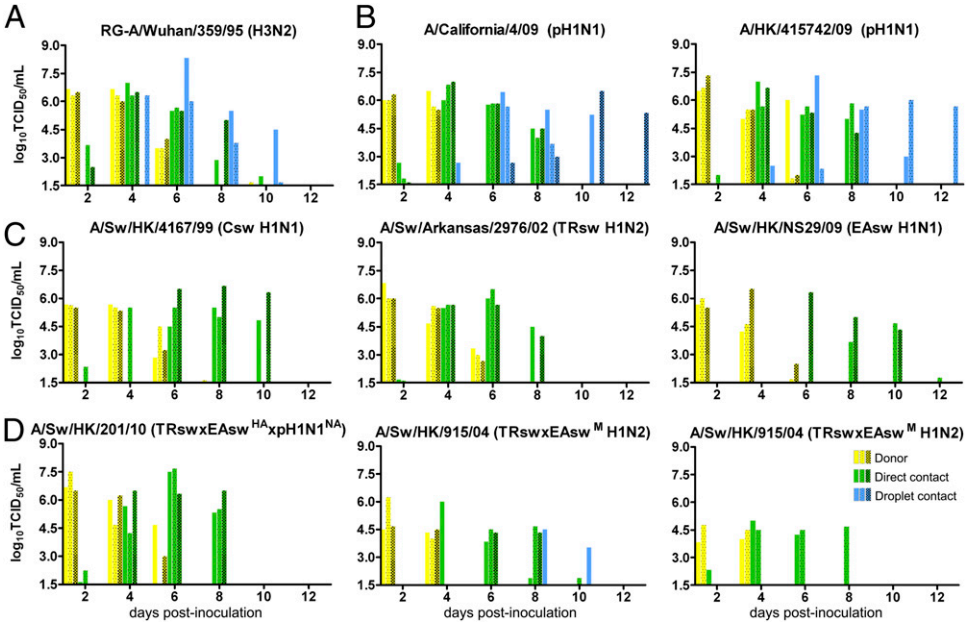

Fig. 1. Transmissibility of seasonal H3N2 (*A*), pandemic H1N1 (*B*), precursor swine (*C*), and reassortant swine (*D*) influenza viruses in ferrets. Values are virus titers ($log_{10}TCID_{50}$/mL) in the nasal washes of individual donor ferrets (yellow), direct contacts (green), and respiratory-droplet contacts (blue). *D* shows experiments for sw915 in two separate panels. The detection limit was $10^{1.5}$ $TCID_{50}$/mL.

MICROBIOLOGY

passages in MDCK cells; however, the full genome sequences of all stock recombinant viruses were verified to be identical to the field isolates. The replication efficiency of RG-sw915 was significantly lower than that of RG-HK415742 at 12 h postinfection in MDCK cells (Fig. 2*B*) ($P < 0.05$, *t* test). The replication efficiency of RG-sw915xHK415742^{PB2,PA} and RG-sw915xHK415742^{NA} did not differ from that of RG-sw915 in MDCK cells. However, the titers of RG-sw915xHK415742^{HA,NA} and RG-sw915xHK415742^{PB2,PA,HA,NA} were comparable to that of RG-HK415742 at 12 h postinoculation, suggesting that the HA of pandemic H1N1 virus conferred efficient replication in MDCK cells. In dNHBE cells, HK415742 replicated to significantly higher titers than sw915 at 48 h postinfection ($P < 0.05$, *t* test); similar trends were observed in RG-HK415742 and RG-sw915 viruses at 24 h and 48 h postinfection ($P < 0.05$, *t* test) (Fig. 2*B*). RG-sw915xHK415742^{NA} and RG-sw915xHK415742^{PB2,PA,HA,NA} viruses replicated to higher titers than did sw915 or RG-swHK915, although the differences did not show statistical significance.

Overall, HK415742 and sw915 differed significantly in replication efficiency in MDCK and dNHBE cells. Replacing the NA of sw915 with that of HK415742 did not improve sw915 replication efficiency. RG-sw915xHK415742^{PB2,PA,HA,NA} showed significantly higher replication efficiency than did RG-sw915 in MDCK cells at 12 h postinfection ($P < 0.05$, *t* test), but the difference was marginal in dNHBE cells.

Transmission of Recombinant Viruses in Ferrets. We evaluated the transmissibility of RG-sw915, RG-sw915xHK415742^{NA}, and RG-sw915xHK415742^{PB2,PA,HA,NA} in ferrets (Fig. 3). The RG-sw915 was transmitted to 3/3 ferrets by direct contact by 4 dpi and to 1/3 ferrets by respiratory droplets by 8 dpi (Fig. 3*A*). Seroconversion was detected in one additional respiratory-droplet contact without detectable virus shedding. Peak titers after direct-contact transmission were detected at 4 or 6 dpi, whereas the peak titer after respiratory-droplet transmission was detected at 8 dpi. Overall, RG-sw915 showed transmissibility comparable to that of the sw915 virus.

Replacing the NA of sw915 with that of HK415742 enhanced respiratory-droplet transmissibility, as the recombinant RG-sw915xHK415742^{NA} virus was transmitted to 3/3 direct contacts by 4 dpi and to 3/3 respiratory-droplet contacts by 8 dpi (Fig. 3*B*). Peak titers were detected consistently from direct contacts at 4 dpi and at 6, 8, and 10 dpi, respectively, from respiratory-droplet contacts. In ferrets inoculated or infected by direct contact with the RG-sw915xHK415742^{NA} virus, the total virus shed (AUC) did not differ from that in the RG-sw915 and sw915 groups (Table S1), suggesting that neither the cumulative amount of virus shed nor the peak viral titers were major contributors to the efficiency of respiratory-droplet transmission.

RG-sw915xHK415742^{PB2,PA,HA,NA} showed more efficient transmissibility than did RG-sw915, as 3/3 direct contacts were infected by 2 dpi and 2/3 respiratory-droplet contacts were infected by 8 dpi (Fig. 3*C*). Peak titers were observed at 4 dpi for all direct contacts and on days 6 and 10 dpi, respectively, for the respiratory-droplet contacts. Whereas animals infected with the RG-sw915xHK415742^{PB2,PA,HA,NA} and RG-sw915 viruses shed a comparable quantity of virus (Table S1), ferrets infected with RG-sw915xHK415742^{PB2,PA,HA,NA} showed more severe clinical signs (lethargy and a croup-like cough was observed in a few infected ferrets) and had a greater increase in body temperature (differences were not statistically significant) (Table S2). These results suggest that higher polymerase activity conferred by PB2 and PA may have contributed to the pathogenicity of the RG-sw915xHK415742^{PB2,PA,HA,NA} virus. Overall, we observed that inserting the NA gene from the pandemic HK415742 virus into sw915 recapitulated the gene constellation of a 2009 pandemic virus and was sufficient to increase respiratory-droplet transmission efficiency in ferrets.

Viral Tropism in the Ferret Respiratory Tract. We evaluated the replication efficiency of the pandemic H1N1 and swine influenza viruses in the ferret respiratory tract on day 3 after inoculation of 10^5 $TCID_{50}$ (*SI Materials and Methods*). The seasonal H3N2 Wuhan95 virus replicated efficiently in the nasal turbinates but only to a limited extent in the conducting airway or the lower lungs (Table S5). The pandemic virus replicated efficiently in both the upper and lower respiratory tracts. The swine influenza viruses were detected in the upper and lower respiratory tracts. Significantly lower titers of the swine viruses than of the pandemic virus were detected in the nasal turbinate (sw915), pharynx (swNS29 and sw915), left bronchi (swNS29), right upper lobe (swNS29 and sw915), and right lower lobe (sw4167, swAR2976, and sw915) ($P < 0.05$) (Table S5). No major histopathologic differences were observed in the respiratory tracts of ferrets inoculated with the pandemic versus swine influenza viruses. Immunohistochemistry revealed viral antigen in bronchial/lung epithelium and bronchial submucosal glands of ferrets inoculated with pandemic H1N1 viruses or swine influenza viruses (Table S6), confirming that these viruses replicate in the ferret lower respiratory tract. Overall, pandemic H1N1 virus and swine influenza viruses showed comparable tissue tropism and replication efficiency in the ferret respiratory tract.

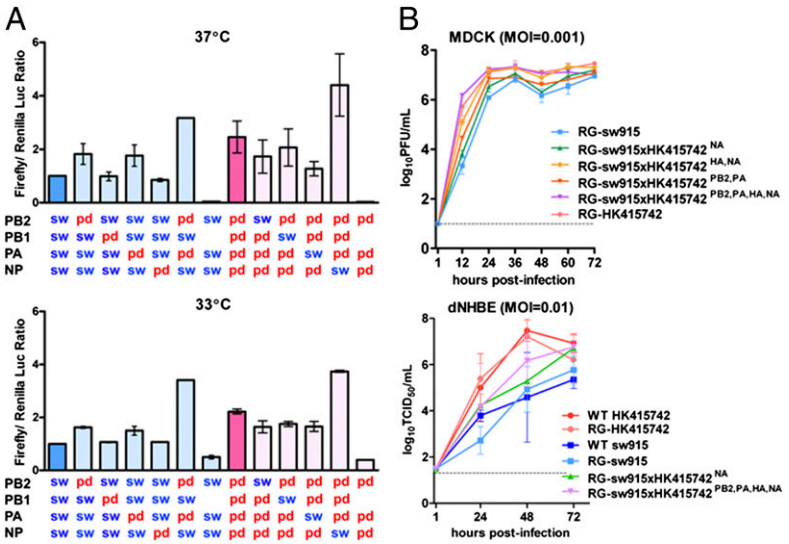

Fig. 2. Polymerase activity and replication efficiency of the recombinant viruses in vitro. (*A*) The transcription and replication efficiency of the polymerase complex of sw915 and HK415742 were evaluated at 37 °C or 33 °C. Values are the mean ± SD from two replicates from independently repeated experiments. (*B*) Viral replication kinetics in MDCK or differentiated NHBE cells were determined at 37 °C at multiplicity of infection (MOI) = 0.001 or 0.01, respectively. Log_{10} mean ± SD values from three replicates (MDCK) or two or three independently performed experiments (NHBE) are shown.

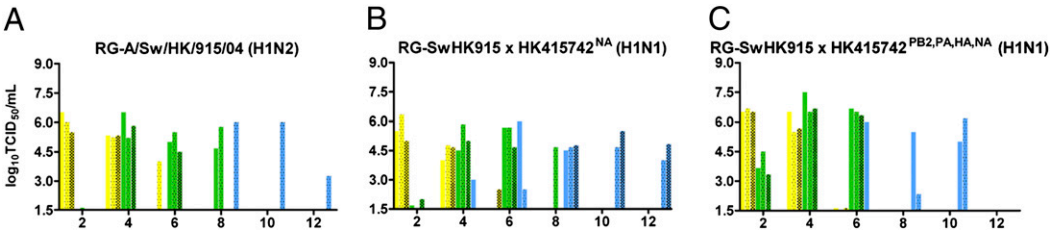

Fig. 3. Transmissibility of the recombinant sw915 viruses in ferrets. The direct-contact and respiratory-droplet transmissibility of RG-sw915 (*A*), RG-sw915xHK415742^{NA} (*B*), and RG-sw915xHK415742^{PB2,PA,HA,NA} (*C*) viruses in ferrets. Viral titers ($log_{10}TCID_{50}$/mL) were obtained from the nasal washes of individual donor ferrets (yellow), direct contacts (green), and respiratory-droplet contacts (blue). The detection limit was $10^{1.5}$ $TCID_{50}$/mL.

Sw915 and HK415742 HA Receptor-Binding Profile by Glycan Array Analysis. Receptor-binding specificity is known to be a molecular determinant of host range and efficient transmissibility (10, 26, 27). Among the 26 amino acids that differed between the HA of sw915 and HK415742 viruses, two residues (219 and 227; H3 numbering) were located in proximity to the 220-loop of the receptor-binding domain (Table S4). We performed glycan array analysis of formalin-fixed sw915 and HK415742 viruses against a panel of 29 α2,3- or α2,6-linked sialosides (16) (Fig. S2). Both sw915 and HK415742 bound preferentially to Neu5Acα2–6Galβ1–4GlcNAc glycans (glycans 23, 27, 28, and 29) (Fig. 4 *A* and *B*), with higher affinity for the longer glycans (28 and 29). The binding affinity of HK415742 and sw915 for these glycans was assayed by using serially diluted sialosides and fitting the data to the Langmuir isotherms by nonlinear regression (*SI Materials and Methods*). The resulting K_d values of the two viruses were comparable for all of the glycans except 27, a sulfated α2,6-linked sialoside (Table S7). Sw915 showed slightly higher binding affinity for glycan 27 than did HK415742. Overall, the results suggest that the HK415742 and sw915 viruses possess comparable receptor-binding specificity and affinity for the identified α2,6-linked sialosides.

NA Enzyme Kinetics. Because replacing the NA of sw915 with that of HK415742 increased transmission efficiency, we compared NA K_M and V_{max} values obtained by using the fluorogenic substrate 2′-(4-methylumbelliferyi)-α-D-*N*-acetylneuraminic acid (MUNANA) and the sialosides 3′SL and 6′SL, which more closely resemble the natural substrates (Fig. 4*C*). To directly compare the activity of NAs from different swine influenza viruses, we generated recombinant PR8 viruses (PR8, PR8xHK415742^{NA}, PR8xsw915^{NA}, PR8xswNS29^{NA}, PR8xswAR2976^{NA}) that differed only in the NA segment. A standardized virus dose of 1.75×10^7 pfu/mL was used. With MUNANA as substrate, the NA of HK415742 showed higher enzyme activity (a higher V_{max}) than the NAs of TRsw-origin (sw915 and swAR2976) and EAsw-origin (swNS29) viruses, despite comparable K_M values (range, 20.5–34.8 μM) (Table 1). HK415742 NA showed similarly higher enzyme activity with the 3′SL or 6′SL substrates; sw915 NA activity was 22% and 29%, respectively, of HK415742 NA activity in catalyzing 3′SL and 6′SL (Table 1 and Fig. 4*C*). HK415742 NA activity was also greater than that of swAR2976 and swNS29 in catalyzing 3′SL or 6′SL. Further, the fitted K_M of the pandemic HK415742 NA in converting 3′SL substrate (336.6 μM) was significantly lower than those of the sw915 or swAR297 NAs (1,831 and 1,017 μM, respectively). As we had observed that sw915 virus possesses a slightly elevated binding affinity for glycan 27 (Table S7), we included glycan 27 in the NA enzyme kinetics studies using wild-type sw915 and HK415742 viruses (1.17×10^6 pfu/mL) after ultrafiltration with an Amicon unit (Millipore). We found that the V_{max} ratio of sw915 relative to HK415742 was only 0.4, whereas the K_M values were comparable between sw915 (2,781 μM) and HK415742 (2,306 μM). Transmission electron microscopy showed viral aggregates in MDCK cells infected with RG-sw915 but not in those infected with RG-sw915xHK415742^{NA}, further supporting the role of HK415742 NA in releasing viral aggregates (Fig. 4 *D* and *E*). Overall, we observed that the NA of the pandemic HK415742 virus possessed higher NA

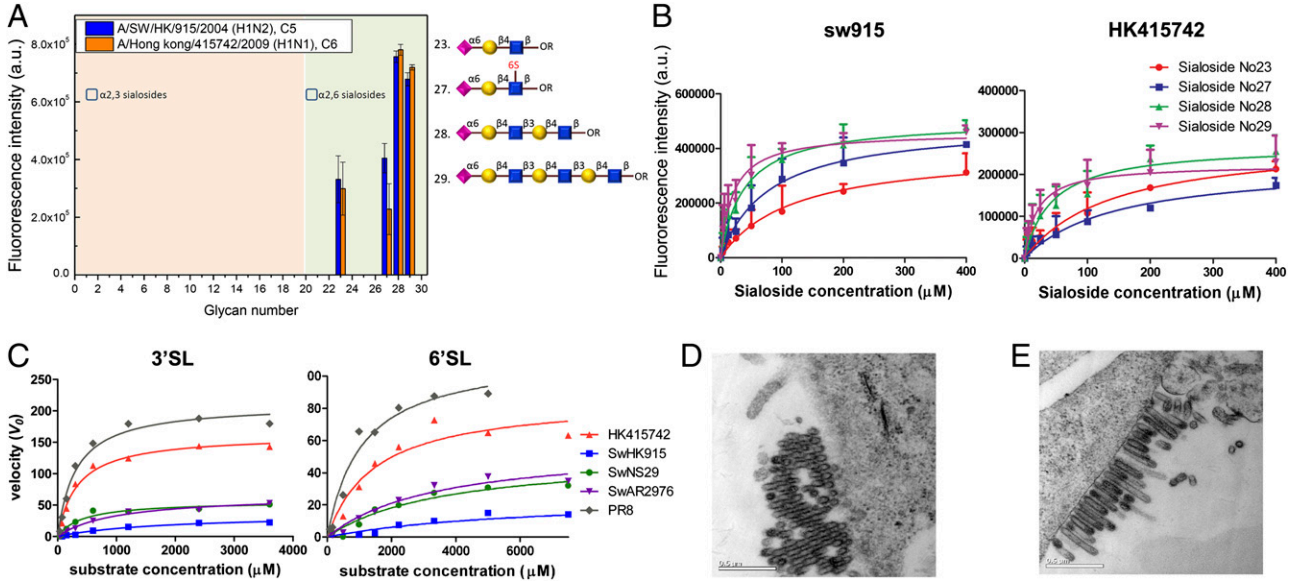

Fig. 4. HA glycan array and NA enzyme kinetics. (*A*) Glycan array analysis of receptor-binding specificity against sialyl glycans (Fig. S1). (*B*) Binding intensity of glycans 23, 27, 28, and 29 with 3×10^6 pfu/mL of HK415742 and sw915 viruses. (*C*) NA enzyme kinetics of recombinant PR8, PR8xHK415742^{NA}, PR8xsw915^{NA}, PR8xswNS29^{NA}, and PR8xswAR2976^{NA} viruses using 3′SL or 6′SL as substrates. The kinetic data were fit to the Michaelis–Menten equation by nonlinear regression to determine the Michaelis constant (K_M) and maximum velocity (V_{max}) of substrate conversion. Transmission electron microscopy shows virus aggregates in MDCK cells infected with RG-sw915 virus (*D*) but not in MDCK cells infected with RG-sw915xHK415742^{NA} virus (*E*) (MOI = 0.1 and fixed after 12 h).

Table 1. NA enzyme kinetics with different substrates

Substrate	Virus	K_M (μM) (95% CI)	V_{max}	R^2	Relative V_{max}
MUNANA	PR8xHK415742^{NA}	29.7 (20.8–38.6)	17.2	0.95	1
	PR8xsw915^{NA}	30.5 (21.8–39.2)	4.0*	0.96	0.23
	PR8xswNS29^{NA}	34.8 (23.1–46.6)	7.2*	0.94	0.42
	PR8xswAR2976^{NA}	20.5 (12.8–28.2)	7.3*	0.91	0.42
	PR8	25.0 (14.9–35.0)	25.0*	0.92	1.45
3′SL	PR8xHK415742^{NA}	336.6 (258.0–415.3)	162.0	0.98	1
	PR8xsw915^{NA}	1,831 (1,016–2,646)*	35.9*	0.98	0.22
	PR8xswNS29^{NA}	432.5 (223.7–641.2)	56.2*	0.94	0.35
	PR8xswAR2976^{NA}	1,017 (691.7–1,342)*	66.4*	0.98	0.41
	PR8	309.3 (219.8–398.8)	211.1*	0.97	1.30
6′SL	PR8xHK415742^{NA}	1,466 (555.4–2,376)	86.1	0.89	1
	PR8xsw915^{NA}	6,112 (0.0–13,723)	25.0*	0.79	0.29
	PR8xswNS29^{NA}	3,642 (594.2–6,691)	51.3	0.88	0.60
	PR8xswAR2976^{NA}	3,452 (1,128–5,777)	57.4	0.91	0.67
	PR8	1,076 (501.6–1,650)	113.8	0.96	1.32

Standardized virus doses were used for the NA kinetics assay. The enzyme kinetics data were fit to the Michaelis–Menten equation by nonlinear regression to determine the Michaelis constant (K_M) and maximum velocity (V_{max}) of substrate conversion. CI, confidence interval.
*$P < 0.05$ compared with PR8xHK415742^{NA}.

activity than the subset of swine influenza viruses tested. This high NA activity may have facilitated the spread and release of virus, thereby conferring efficient transmissibility.

Discussion

Although the immediate precursor of the 2009 pandemic virus has not been identified, our 13-y surveillance of swine influenza viruses provided representatives of the Csw, TRsw, and EAsw lineages (which donated gene segments to the pandemic virus) and natural reassortants between these lineages (2, 24, 25). Using a ferret model to analyze the transmission potential of a representative subset of swine influenza isolates before 2009, we confirmed that they are not transmitted via respiratory droplets, with the exception of sw915, which is inefficiently transmitted by this route. This finding is consistent with the epidemiological data in humans.

The sw915 virus is a TRsw-like virus that has acquired the M gene from the EAsw lineage through reassortment. This genotype was isolated only once in southern China during the 13-y surveillance period (25), suggesting that its specific gene constellation is not well-adapted in swine. However, additional sw915-like viruses have been isolated more recently in southern China by our surveillance system. It remains to be determined whether the recent sw915-like isolates have an improved fitness in the swine host. The M genes of sw915 and HK415742 encode an identical M1 protein, but their M2 proteins differ by seven amino acids. The inefficient droplet transmissibility of the sw915 virus suggests that the gene constellation of sw915 may contain some of the necessary determinants (including the Eurasian-derived M gene) of respiratory-droplet transmissibility. Introducing the NA gene from the pandemic HK415742 into the sw915 virus by reverse genetics recapitulated the gene constellation of a 2009 pandemic virus and conferred efficient respiratory-droplet transmissibility. The high NA activity observed in the pandemic H1N1 virus may facilitate virus release and spread. However, the lack of respiratory-droplet transmission of sw201 (which acquired the pandemic NA gene through natural reassortment) indicated that the NA gene alone is not sufficient to confer respiratory-droplet transmission. Overall, our results suggest that a specific gene constellation and balanced HA–NA activity are critical factors for efficient respiratory-droplet transmission. Future work will analyze the interaction between surface glycoproteins and M1 to further characterize the relation of surface glycoprotein expression level to respiratory-droplet transmissibility.

Viral receptor-binding specificity and cell tropism in the human airway were hypothesized to be key determinants of efficient transmission (28). However, recent reports show that the swine influenza viruses and the 2009 pandemic viruses possess similar receptor-binding specificity for α2,6-linked sialosides (17, 22), suggesting that differences between the swine and pandemic HAs were not the key determinants of respiratory-droplet transmissibility of the 2009 pandemic virus. We also found that pandemic HK415742 and sw915 viruses possessed similar receptor-binding specificity and affinity for α2,6-linked sialosides. The HA of the two viruses differed by 26 amino acids, including residues 219 and 227 located at the 220-loop of the receptor-binding domain. Like H1 seasonal influenza virus, the pandemic viruses possess E227 in HA, whereas the majority of the H1 swine influenza viruses possess A227. Similarly, I219 is unique in pandemic H1N1 viruses; A/T219 is commonly seen in swine influenza HA. The comparable HA-binding specificity and affinity of HK415742 and sw915 against a panel of 29 synthetic sialosides suggest that these two residues played a minor role in determining receptor recognition.

Both HA and NA recognize sialosides, but with counteracting functions. Whereas we found no evidence that HA alone played a role in acquisition of respiratory-droplet transmissibility, we observed that introducing the NA from pandemic HK415742 into sw915 conferred efficient respiratory-droplet transmissibility. There was also a significant difference in NA enzyme activity between HK415742 and sw915 in catalyzing MUNANA, 3′SL, 6′SL, or a sulfated α2,6-linked sialoside identified by glycan array. The sw915 NA V_{max} was only 22% and 29%, respectively, of the HK415742 NA V_{max} in catalyzing 3′SL and 6′SL. Recent human N2 viruses have been observed to have higher NA enzyme activity for α2,6-linked sialosides than do avian or early human N2 viruses (29). Our findings suggest that high NA activity is associated with the efficient respiratory-droplet transmission of the pandemic H1N1 virus; however, it is not clear whether high NA activity is required for the initiation of infection, the egress and spread of virus, or both. Absence of efficient respiratory-droplet transmission in the sw201 virus, a natural reassortant that possesses an EAsw HA and a pandemic H1N1 NA, suggests that optimal HA–NA balance is required for efficient human-to-human transmission.

Human influenza polymerase protein PB2 was reported to be one of the molecular determinants of efficient respiratory-droplet transmission of an avian influenza virus isolated from mallards (13). Using a minigenome assay, we observed that HK415742 possessed twice the transcription/replication efficiency of sw915 and that this higher activity was conferred by its PB2 and PA. RG-sw915xHK415742^{PB2,PA,HA,NA} virus replicated to higher titers than RG-sw915 virus in MDCK ($P < 0.05$) and differentiated NHBE cells. However, RG-sw915xHK415742^{PB2,PA,HA,NA} did not show better replication efficiency than RG-sw915 in nasal washes or tissues of the respiratory tract at 3 dpi, although ferrets infected with the RG-sw915xHK415742^{PB2,PA,HA,NA} virus showed more severe clinical signs. In our experimental setting, pandemic-derived PB2 and PA did not enhance the respiratory-droplet transmissibility of sw915. As the PB2 and PA of sw915 and HK415742 belong to the same phylogeny, which derives from TRsw-like viruses, it is possible that the determinants of efficient transmission reside in their common residues. The PB2 S590/R591 residues, which may have facilitated adaptation of the 2009 pandemic influenza virus to humans (26), are shared by the sw915 and HK415742 viruses. Future studies may apply EAsw-derived polymerase proteins or site-directed mutagenesis of the PB2 S590/R591 residues to further elucidate the role of polymerase proteins in conferring respiratory-droplet transmission.

Our results highlight the importance of swine influenza viruses, all of which are transmissible by direct contact in ferrets and can easily cross the species barrier, as a potential source of future pandemics. Others have previously used animal models to study the transmissibility of the pandemic H1N1 virus in comparison with human seasonal influenza viruses or TRsw-like swine influenza viruses (30–33). Our approach of using field swine isolates followed by the generation of recombinant viruses allowed us to more closely approximate the events that led to the emergence of the 2009 pandemic H1N1 virus with its efficient transmissibility in humans.

The 2009 pandemic emerged without warning, caused by a novel reassortant that had not previously been recognized as a potential pandemic pathogen. There is a critical need to identify biological markers that may predict the risk of transmissibility of animal viruses to, and among, humans. Neither the viral polymerase activity (minigenome assays) nor the intensity of viral replication (peak titers, AUC) in ferrets were good correlates of transmission potential. As viral determinants of transmission are polygenic, virus replication efficiency in the upper respiratory tract is likely only one of multiple determining factors. Other viral factors may include the ability to infect and to release from mucin, virus aerosolization efficiency, the ability to induce sneezing, or the ability to evade the host innate response. Here we demonstrate that respiratory-droplet transmission in ferrets is a good correlate of the acquisition of transmissibility in humans. In the context of enhanced global surveillance of swine influenza viruses, respiratory-droplet transmission in ferrets could provide a tool for human health risk assessment and contribute to global pandemic preparedness.

Materials and Methods

Transmission Experiments in Ferrets. Transmissibility was tested in 4- to 6-mo-old male ferrets obtained from Triple F Farms. All studies were conducted in a Biosafety Level 2+ facility at St. Jude Children's Research Hospital in compliance with all applicable laws and guidelines and with the approval of the St. Jude Children's Research Hospital Animal Care and Use Committee. Ferrets used in the study were confirmed to have an hemagglutination inhibition titer ≤40 against pandemic influenza H1N1 (A/TN/560/2009), human seasonal H3N2 (A/Brisbane/10/2007), and influenza B (B/Florida/4/2006). Virus transmission experiments used groups of three inoculated ferrets, three naïve direct-contact ferrets, and three naïve respiratory droplet-contact ferrets. Donors were inoculated intranasally with 10^5 $TCID_{50}$ of virus in 0.5 mL media under isoflurane anesthesia. After 1 d, a naïve direct-contact ferret was placed in the same cage with each inoculated ferret, and one naïve respiratory droplet-contact ferret was placed in an adjacent compartment of the cage, separated by a double-layered perforated divider. To monitor virus shedding, nasal washes and rectal swabs were collected from all ferrets every other day for 14 d and titrated in MDCK cells. The AUC was calculated by using GraphPad Prism software. Ferret weight, temperature, and clinical signs were monitored daily. Naïve respiratory droplet-contact ferrets were handled before naïve direct-contact ferrets, and inoculated ferrets were handled last; hands and equipment were disinfected before and after handling each ferret. Separate gloves and tools were used for respiratory droplet-contact ferrets. Seroconversion was monitored by titrating virus-neutralizing antibody in sera collected before and 18–21 d after placement in shared housing.

NA Kinetics. NA kinetics studies used recombinant PR8, PR8xHK415742^{NA}, PR8xsw915^{NA}, PR8xswNS29^{NA}, and PR8xswAR2976^{NA} viruses at 1.75×10^7 pfu/mL; M gene copy number was determined by quantitative real-time PCR to ensure comparable virus doses. NA kinetics using MUNANA were determined at a final concentration of 0–400 μM at 37 °C in a total volume of 50 μL. The fluorescence of the released 4-methylumbelliferone was measured every 68 s for 45 min by using FLUOstar OPTIMA (BMG Labtech) with excitation and emission wavelengths of 355 and 460 nm, respectively. NA kinetics using 3′SL, 6′SL (Carbosynth), or glycan 27 (Genomic Research Center, Academia Sinica) substrates were determined by a coupled enzyme assay. Viruses were incubated with 3′SL (final concentration, 0–4,500 μM) or 6′SL (final concentration, 0–11,500 μM) at pH 6.0 with 0.2 M phosphate buffer, excess galactose oxidase (Sigma-Aldrich), horseradish peroxidase (Invitrogen), and Amplex UltraRed reagent (Invitrogen). The reaction was conducted at 37 °C and the fluorogenic product was measured every 5 min for 6–10 h using FLUOstar OPTIMA with excitation and emission wavelengths of 530 and 590 nm, respectively. The enzyme kinetics data were fitted to the Michaelis–Menten equation by using nonlinear regression (Prism; GraphPad) to determine the Michaelis constant (K_M) and maximum velocity (V_{max}) of substrate conversion.

ACKNOWLEDGMENTS. We thank Dr. K. H. Chan for providing the pandemic H1N1 virus; Drs. G. J. D. Smith and D. Vijaykrishna for informative discussions; E. S. K. Ma, H. P. Chiu, and C. S. W. Leung, P. Seiler, K. Friedman, J. Franks, J. Turner, J. C. Crumpton, B. Marathe, A. Prevost, and D. Carey for technical assistance; and S. Naron for manuscript editing. This study was supported by the Research Fund for the Control of Infectious Diseases Commissioned Project from the Food and Health Bureau, Hong Kong; the Area of Excellence Scheme of the University Grants Committee (AoE/M-12/06), Hong Kong; Seed Funding for Basic Research, University of Hong Kong; and Contract HHSN266200700005C from the National Institute of Allergy and Infectious Diseases, National Institutes of Health.

1. Garten RJ, et al. (2009) Antigenic and genetic characteristics of swine-origin 2009 A(H1N1) influenza viruses circulating in humans. *Science* 325:197–201.
2. Smith GJ, et al. (2009) Origins and evolutionary genomics of the 2009 swine-origin H1N1 influenza A epidemic. *Nature* 459:1122–1125.
3. Zhou NN, et al. (1999) Genetic reassortment of avian, swine, and human influenza A viruses in American pigs. *J Virol* 73:8851–8856.
4. Vincent AL, Ma W, Lager KM, Janke BH, Richt JA (2008) Swine influenza viruses: A North American perspective. *Adv Virus Res* 72:127–154.
5. Donatelli I, et al. (1991) Detection of two antigenic subpopulations of A(H1N1) influenza viruses from pigs: Antigenic drift or interspecies transmission? *J Med Virol* 34:248–257.
6. Scholtissek C, Bürger H, Bachmann PA, Hannoun C (1983) Genetic relatedness of hemagglutinins of the H1 subtype of influenza A viruses isolated from swine and birds. *Virology* 129:521–523.
7. Myers KP, Olsen CW, Gray GC (2007) Cases of swine influenza in humans: A review of the literature. *Clin Infect Dis* 44:1084–1088.
8. Shinde V, et al. (2009) Triple-reassortant swine influenza A (H1) in humans in the United States, 2005–2009. *N Engl J Med* 360:2616–2625.
9. Karasin AI, et al. (2000) Genetic characterization of H3N2 influenza viruses isolated from pigs in North America, 1977–1999: Evidence for wholly human and reassortant virus genotypes. *Virus Res* 68:71–85.
10. Tumpey TM, et al. (2007) A two-amino acid change in the hemagglutinin of the 1918 influenza virus abolishes transmission. *Science* 315:655–659.
11. Pappas C, et al. (2010) Receptor specificity and transmission of H2N2 subtype viruses isolated from the pandemic of 1957. *PLoS One* 5:e11158.
12. Steel J, Lowen AC, Mubareka S, Palese P (2009) Transmission of influenza virus in a mammalian host is increased by PB2 amino acids 627K or 627E/701N. *PLoS Pathog* 5: e1000252.
13. Van Hoeven N, et al. (2009) Human HA and polymerase subunit PB2 proteins confer transmission of an avian influenza virus through the air. *Proc Natl Acad Sci USA* 106: 3366–3371.
14. Herfst S, et al. (2010) Introduction of virulence markers in PB2 of pandemic swine-origin influenza virus does not result in enhanced virulence or transmission. *J Virol* 84: 3752–3758.
15. Zhu H, et al. (2010) Substitution of lysine at 627 position in PB2 protein does not change virulence of the 2009 pandemic H1N1 virus in mice. *Virology* 401:1–5.
16. Liao HY, et al. (2010) Differential receptor binding affinities of influenza hemagglutinins on glycan arrays. *J Am Chem Soc* 132:14849–14856.
17. Chen LM, et al. (2011) Receptor specificity of subtype H1 influenza A viruses isolated from swine and humans in the United States. *Virology* 412:401–410.
18. Childs RA, et al. (2009) Receptor-binding specificity of pandemic influenza A (H1N1) 2009 virus determined by carbohydrate microarray. *Nat Biotechnol* 27:797–799.
19. Liu Y, et al. (2010) Altered receptor specificity and cell tropism of D222G hemagglutinin mutants isolated from fatal cases of pandemic A(H1N1) 2009 influenza virus. *J Virol* 84:12069–12074.
20. Ito T, et al. (1998) Molecular basis for the generation in pigs of influenza A viruses with pandemic potential. *J Virol* 72:7367–7373.
21. Rogers GN, D'Souza BL (1989) Receptor binding properties of human and animal H1 influenza virus isolates. *Virology* 173:317–322.
22. Bateman AC, et al. (2010) Glycan analysis and influenza A virus infection of primary swine respiratory epithelial cells: The importance of NeuAcα2-6 glycans. *J Biol Chem* 285:34016–34026.
23. Mehle A, Doudna JA (2009) Adaptive strategies of the influenza virus polymerase for replication in humans. *Proc Natl Acad Sci USA* 106:21312–21316.
24. Vijaykrishna D, et al. (2010) Reassortment of pandemic H1N1/2009 influenza A virus in swine. *Science* 328:1529.
25. Vijaykrishna D, et al. (2011) Long-term evolution and transmission dynamics of swine influenza A virus. *Nature* 473:519–522.
26. Belser JA, Maines TR, Tumpey TM, Katz JM (2010) Influenza A virus transmission: Contributing factors and clinical implications. *Expert Rev Mol Med* 12:e39.
27. Neumann G, Kawaoka Y (2006) Host range restriction and pathogenicity in the context of influenza pandemic. *Emerg Infect Dis* 12:881–886.
28. Shinya K, et al. (2006) Avian flu: Influenza virus receptors in the human airway. *Nature* 440:435–436.
29. Kobasa D, et al. (1999) Amino acid residues contributing to the substrate specificity of the influenza A virus neuraminidase. *J Virol* 73:6743–6751.
30. Belser JA, et al. (2011) Pathogenesis and transmission of triple-reassortant swine H1N1 influenza viruses isolated before the 2009 H1N1 pandemic. *J Virol* 85:1563–1572.
31. Maines TR, et al. (2009) Transmission and pathogenesis of swine-origin 2009 A(H1N1) influenza viruses in ferrets and mice. *Science* 325:484–487.
32. Munster VJ, et al. (2009) Pathogenesis and transmission of swine-origin 2009 A(H1N1) influenza virus in ferrets. *Science* 325:481–483.
33. Steel J, Palese P, Lowen AC (2010) Transmission of a 2009 pandemic influenza virus shows a sensitivity to temperature and humidity similar to that of an H3N2 seasonal strain. *J Virol* 85:1400–1402.